eNeuro

Research Article: New Research | Novel Tools and Methods

Rostrocaudal Areal Patterning of Human PSC-Derived Cortical Neurons by FGF8 Signaling

Kent Imaizumi¹, Koki Fujimori^{1,2}, Seiji Ishii¹, Asako Otomo³, Yasushi Hosoi⁴, Hiroaki Miyajima⁴, Hitoshi Warita⁵, Masashi Aoki⁵, Shinji Hadano³, Wado Akamatsu^{1,6} and Hideyuki Okano¹

¹Department of Physiology, Keio University School of Medicine, 35 Shinanomachi, Shinjuku, Tokyo 160-8582, Japan

²Research Fellow of Japan Society for the Promotion of Science, 5-3-1, Kojimachi, Chiyoda, Tokyo 102-0083, Japan

³Department of Molecular Life Sciences, Tokai University School of Medicine, 143 Shimokasuya, Isehara, 259-1193, Japan

⁴First Department of Medicine, Hamamatsu University School of Medicine, 1-20-1, Handayama, Hamamatsu, 431-3192, Japan

⁵Department of Neurology, Tohoku University Graduate School of Medicine, 1-1 Seiryo-Machi, Aoba-Ku, Sendai 980-8574, Japan

⁶Center for Genomic and Regenerative Medicine, Juntendo University School of Medicine, 2-1-1 Hongo, Bunkyoku, Tokyo 113-8421, Japan

DOI: 10.1523/ENEURO.0368-17.2018

Received: 27 October 2017

Revised: 8 April 2018

Accepted: 9 April 2018

Published: 13 April 2018

Author contribution: KI, WA, and HO designed research; KI, SI, and AO performed research; AO, YH, HM, HW, MA, and SH contributed unpublished reagents; KI and KF analyzed data; KI, WA, and HO wrote the paper.

H.O. serves as a paid scientific advisor to SanBio Co. Ltd. and K Pharma Inc. The remaining authors declare no competing financial interests.

Correspondence should be addressed to either Wado Akamatsu, Center for Genomic and Regenerative Medicine, Juntendo University School of Medicine, 2-1-1 Hongo, Bunkyoku, Tokyo 113-8421, Japan, or Hideyuki Okano, Department of Physiology, Keio University School of Medicine, 35 Shinanomachi, Shinjuku, Tokyo 160-8582, Japan. E-mail: awado@juntendo.ac.jp or hidokano@a2.keio.jp

Cite as: eNeuro 2018; 10.1523/ENEURO.0368-17.2018

Alerts: Sign up at eneuro.org/alerts to receive customized email alerts when the fully formatted version of this article is published.

Accepted manuscripts are peer-reviewed but have not been through the copyediting, formatting, or proofreading process.

Copyright © 2018 Imaizumi et al.

This is an open-access article distributed under the terms of the Creative Commons Attribution 4.0 International license, which permits unrestricted use, distribution and reproduction in any medium provided that the original work is properly attributed.

1 **Title**

2 Rostrocaudal Areal Patterning of Human PSC-Derived Cortical Neurons by FGF8

- 3 Signaling
- 4

5 Abbreviated title

6 Areal Patterning in PSC Culture by FGF8

7

8 Authors

- 9 Kent Imaizumi¹, Koki Fujimori^{1,2}, Seiji Ishii¹, Asako Otomo³, Yasushi Hosoi⁴, Hiroaki
- 10 Miyajima⁴, Hitoshi Warita⁵, Masashi Aoki⁵, Shinji Hadano³, Wado Akamatsu^{1, 6}, and
- 11 Hideyuki Okano¹.

12

- ¹Department of Physiology, Keio University School of Medicine, 35 Shinanomachi,
- 14 Shinjuku, Tokyo 160-8582, Japan
- ¹⁵ ²Research Fellow of Japan Society for the Promotion of Science, 5-3-1, Kojimachi,
- 16 Chiyoda, Tokyo, 102-0083, Japan.
- ³Department of Molecular Life Sciences, Tokai University School of Medicine, 143
- 18 Shimokasuya, Isehara 259-1193, Japan
- ⁴First Department of Medicine, Hamamatsu University School of Medicine, 1-20-1,
- 20 Handayama, Hamamatsu, 431-3192, Japan
- 21 ⁵Department of Neurology, Tohoku University Graduate School of Medicine, 1-1
- 22 Seiryo-machi, Aoba-ku, Sendai 980-8574, Japan
- 23 ⁶Center for Genomic and Regenerative Medicine, Juntendo University School of
- 24 Medicine, 2-1-1 Hongo, Bunkyoku, Tokyo 113-8421, Japan

25

26 Author Contribution

- 27 KI, WA, and HO designed research; KI, SI, and AO performed research; AO, YH, HM,
- 28 HW, MA, and SH contributed unpublished reagents; KI and KF analyzed data; KI, WA,

and HO wrote the paper.

30

31 Correspondence

- 32 Correspondence should be addressed to either Dr. Wado Akamatsu, Center for Genomic
- 33 and Regenerative Medicine, Juntendo University School of Medicine, 2-1-1 Hongo,

- 34 Bunkyoku, Tokyo 113-8421, Japan, or Dr. Hideyuki Okano, Department of Physiology,
- 35 Keio University School of Medicine, 35 Shinanomachi, Shinjuku, Tokyo 160-8582,
- 36 Japan. E-mail: awado@juntendo.ac.jp or hidokano@a2.keio.jp.
- 37
- 38 Number of figures: 4
- 39 Number of tables: 0
- 40 Number of multimedia: 0
- 41 Number of words for Abstract, Significance Statement, Introduction, and Discussion:
- 42 114, 108, 493, 801 respectively.
- 43

44 Acknowledgments

45 This study was supported by grants from the New Energy and Industrial Technology

- 46 Development Organization, the Ministry of Education, Science, Sports and Culture
- 47 (MEXT) of Japan, and the Ministry of Health, Labour and Welfare (MHLW) of Japan
- 48 to H.O. and W.A.; by the Program for Intractable Disease Research Utilizing
- 49 Disease-Specific iPS Cells funded by the Japan Science and Technology Agency
- 50 (JST)/Japan Agency for Medical Research and Development (AMED) to H.O. and
- 51 W.A.; by the Practical Research Project for Rare/Intractable Diseases by AMED to H.O
- 52 and M.A; by the Ice Bucket Challenge Grant from Japan ALS Association to H.O.; and
- 53 by Keio University Research Grants for Life Science and Medicine to K.I. We are
- 54 grateful to N. Nakatsuji and H. Suemori (Kyoto University) for ESCs; S. Yamanaka
- 55 (Kyoto University) for control iPSCs; and all members of the H.O. laboratory for
- 56 encouragement and kind support.
- 57

58 **Conflict of interest**

- 59 H.O. serves as a paid scientific advisor to SanBio Co. Ltd. and K Pharma Inc. The
- 60 remaining authors declare no competing financial interests.
- 61
- 62
- 63

64 Abstract

65	The cerebral cortex is subdivided into distinct areas that have particular functions. The
66	rostrocaudal (R-C) gradient of fibroblast growth factor 8 (FGF8) signaling defines this
67	areal identity during neural development. In this study, we recapitulated cortical R-C
68	patterning in human pluripotent stem cell (PSC) cultures. Modulation of FGF8 signaling
69	appropriately regulated the R-C markers, and the patterns of global gene expression
70	resembled those of the corresponding areas of human fetal brains. Furthermore, we
71	demonstrated the utility of this culture system in modeling the area-specific forebrain
72	phenotypes (presumptive upper motor neuron (UMN) phenotypes) of amyotrophic
73	lateral sclerosis (ALS). We anticipate that our culture system will contribute to studies
74	of human neurodevelopment and neurological disease modeling.
75	

76 Significance Statement

- 77 Although the cerebral cortex is organized into functionally unique subdivisions or areas,
- 78 the areal specification has not been studied extensively in PSC-based
- 79 neurodevelopmental models. Here, we report a culture system to control the areal
- 80 identity of PSC-derived cerebral cortical progenitors along the R-C axis by modulating
- 81 FGF8 signaling. Treatment with FGF8 conferred rostral (the sensorimotor cortex)
- 82 identity on cerebral cortical progenitors, whereas these progenitors retained caudal (the
- 83 temporal lobe) identity in the absence of FGF8. By using this culture system, we
- 84 succeeded in modeling area-specific forebrain phenotypes (presumptive UMN
- 85 phenotypes) of ALS. This system offers a novel platform in the field of human
- 86 neurodevelopment and neurological disease modeling.

88 Introduction

89	The cerebral cortex has a pivotal role in higher-order brain functions in humans. It is
90	divided into discrete, specialized subdomains called areas, and its complex
91	information-processing capability is a function of neuronal computation performed
92	across these areas. Areal identity is initially defined during neural development and is
93	driven by morphogens that are secreted from patterning centers (O'Leary et al., 2007).
94	For instance, it has been demonstrated that the rostrocaudal (R-C) gradient of fibroblast
95	growth factor 8 (FGF8) secreted from the anterior neural ridge (ANR) patterns the
96	cortical areas (Fukuchi-Shimogori and Grove, 2001). However, the mechanism of areal
97	patterning has mostly been studied in mouse models, and it is unclear whether the
98	findings can be applied to human cerebral cortex development.
99	It is difficult to study human neurodevelopment using human neural cells directly
100	taken from embryos because this process is ethically and technically restricted. To
101	overcome these limitations, researchers now take advantage of human pluripotent stem
102	cells (PSCs), including embryonic stem cells (ESCs) and induced PSCs (iPSCs). These
103	cells have the potential to differentiate into various neural subtypes and offer in vitro

104	models to study the developmental process in humans (Tao and Zhang, 2016). Indeed,
105	human PSCs can recapitulate the regional patterning of various brain regions, including
106	the forebrain, the midbrain, the hindbrain, and the spinal cord (Kadoshima et al., 2013;
107	Maroof et al., 2013; Imaizumi et al., 2015; Lippmann et al., 2015; Lu et al., 2015;
108	Muguruma et al., 2015). In this way, PSCs provide a promising tool to study human
109	cerebral cortical area patterning. However, cortical areal identity in PSC cultures has
110	not been extensively studied.
111	PSCs also have a remarkable potential to serve as in vitro models of neurological
112	diseases. Given that it is difficult to obtain patient-derived neural cells or tissues
113	because of the limited accessibility of the brain, PSC-based recapitulation of disease
114	phenotypes is an attractive tool for clarifying pathogenesis. When modeling
115	neurological diseases with PSCs, it is necessary to generate neural cells with
116	appropriate regional identities because most neurological diseases preferentially affect
117	specific brain regions (Mattis and Svendsen, 2011; Marchetto and Gage, 2012;
118	Imaizumi and Okano, 2014; Okano and Yamanaka, 2014). In terms of diseases that
119	affect the cortex, specific areas are often selectively damaged; for example, the motor

120	cortex is a prime target in amyotrophic lateral sclerosis (ALS). Therefore, the
121	technology to control the areal identity of PSC-derived cortical neurons will also be
122	helpful for in vitro modeling of neurological diseases.
123	Here, we report a PSC-based culture system that models control of the areal identity
124	of cerebral cortical progenitors along the R-C axis by modulating FGF8 signaling. The
125	control of R-C identity was confirmed by analyzing the expression of the R-C markers
126	and by comparing their transcriptome with that of human fetal brains. Furthermore, we
127	detected area-specific forebrain phenotypes (presumptive upper motor neuron (UMN)
128	phenotypes) of ALS by using this culture system. Our work opens up new opportunities
129	for studies of human neurodevelopment and neurological disease modeling.
130	

131 Materials and Methods

- 132 Generation and culture of undifferentiated ESCs and iPSCs. Human ESCs (KhES-1,
- 133 46XX) (Suemori et al., 2006), control human iPSCs (201B7, 46XX) (Takahashi et al.,
- 134 2007), FUS-mutated iPSCs (FALS-e46, 46XY) (Ichiyanagi et al., 2016), and
- 135 ALS2-mutated iPSCs (4605, 46XY) were used in this study. We generated
- 136 ALS2-mutated iPSCs from a patient with familial ALS (ALS2) (Shirakawa et al., 2009)
- 137 as previously described (Seki et al., 2010). These cells were cultured on SNL murine
- 138 fibroblast feeder cells in standard human ESC medium in an atmosphere containing 3%
- 139 CO₂ (Imaizumi et al., 2015).
- 140 ESCs were used in accordance with the guidelines regarding the utilization of
- 141 human ESCs, with approval from the Ministry of Education, Culture, Sports, Science,
- 142 and Technology (MEXT) of Japan and the Keio University School of Medicine Ethics
- 143 Committee. All experimental procedures for iPSCs derived from patients were
- 144 approved by the Keio University School of Medicine Ethics Committee (approval no.

145 20080016).

147	Neuronal induction. Neuronal induction of ESCs/iPSCs was performed by using the
148	neurosphere culture system as previously described (Imaizumi et al., 2015) with slight
149	modifications. Briefly, ESCs/iPSCs were pretreated for 6 days with 3 μM SB431542
150	(Tocris) and 150 nM LDN193189 (StemRD). They were then dissociated and seeded at
151	a density of 10 cells/ μ L in media hormone mix (MHM) (Shimazaki et al., 2001; Okada
152	et al., 2004, 2008) with selected growth factors and inhibitors under conditions of 4%
153	$O_2/5\%$ CO_2. The growth factors and inhibitors included 20 ng/mL FGF-2, 1× B27
154	supplement without vitamin A (Invitrogen), 2 μM SB431542, 10 μM Y-27632
155	(Calbiochem), and 3 μM IWR-1e (Calbiochem). Defining the day on which
156	neurosphere culture was started as day 0, cells were reseeded at 50 cells/ μ L in MHM
157	with 1× B27 and 10 μM Y-27632 on day 12. The following patterning factors were also
158	added on day 12: 50-200 ng/mL FGF8 (Peprotech) and 100 ng/mL soluble FGFR3
159	(Peprotech). On day 18, neurospheres were replated en bloc on coverslips coated with
160	poly-ornithine and laminin and cultured under conditions of 5% CO ₂ . The medium was
161	changed to MHM supplemented with $1 \times B27$.

162	For LMN induction, pretreated PSCs were seeded at 10 cells/ μ L in MHM with 20
163	ng/mL FGF-2, 1× B27, 2 μM SB431542, 10 μM Y-27632, and 3 μM CHIR99021
164	(Stemgent), 1 μM retinoic acid (Sigma) under conditions of 4% $O_2/5\%$ CO_2. On day 2,
165	100 ng/mL Shh-C24II (R&D Systems) and 1 μM purmorphamine (Calbiochem) were
166	added. On day 6, cells were reseeded at 10-50 cells/ μ L in MHM with 20 ng/mL FGF-2,
167	$1\times$ B27, 10 μM Y-27632, 1 μM retinoic acid, and 1 μM purmorphamine. On day 12,
168	neurospheres were replated and cultured under conditions of 5% CO ₂ . The medium was
169	changed to MHM supplemented with 1× B27 and 1 μM DAPT (Sigma).
170	
171	Quantitative RT-PCR. Total RNA was isolated with the RNeasy Mini Kit (Qiagen) with
172	DNase I treatment, and cDNA was prepared by using a ReverTraAce qPCR RT Kit
173	(Toyobo). The qRT-PCR analysis was performed with SYBR premix Ex Taq II (Takara
174	Bio) on a ViiA 7 Real-Time PCR System (Applied Biosystems). Values were
175	normalized to ACTB. Reactions were carried out in duplicate, and data were analyzed
176	by using the comparative ($\Delta\Delta$ Ct) method. Relative expression levels are presented as
177	

- 179 5'-GGAGGAGCAATGATCTTGAT-3'; SP8, forward
- 180 5'-TTCTAGGGCGTGGTGCTTG-3', reverse 5'-GAAGAGGACGAGGAGCGTTT-3';
- 181 PEA3, forward 5'-CTCGCTCCGATACTATTATG-3', reverse
- 182 5'-CTCATCCAAGTGGGACAAAG-3'; COUP-TFI, forward
- 183 5'-AAGCCATCGTGCTGTTCAC-3', reverse 5'-GCTCCTCACGTACTCCTCCA-3';
- and *FGFR3*, forward 5'-GCCTCCTCGGAGTCCTTG-3', reverse
- 185 5'-CGAAGACCAACTGCTCCTG-3'.
- 186
- 187 Immunocytochemistry. Cells were fixed with 4% paraformaldehyde for 15 min at room
- 188 temperature and then washed three times with PBS. After incubating with blocking
- 189 buffer (PBS containing 5% normal fetal bovine serum and 0.3% Triton X-100) for 1 h
- 190 at room temperature, the cells were incubated for 1-2 days at 4°C with primary
- 191 antibodies at the following dilutions: cleaved CASPASE3 (rabbit, CST, 9661, 1:500),
- 192 COUP-TFI (mouse, Perseus, PP-H8132-00, 1:1000), CTIP2 (rat, Abcam, ab18465,
- 193 1:200), HB9 (mouse IgG1, DSHB, 81.5C10, 1:250), FOXP2 (goat, Santa Cruz,

194	sc-21069, 1:500), OTX1 (mouse, DSHB, 5F5, 1:5000), SOX1 (goat, R&D, AF3369,
195	1:500), SP8 (goat, Santa Cruz, sc-104661, 1:500), and β III-tubulin (mouse IgG2b,
196	Sigma, T8660, 1:500). The cells were again washed three times with PBS and incubated
197	with secondary antibodies conjugated with Alexa Fluor 488, Alexa Fluor 555, or Alexa
198	Fluor 647 (Life Technologies) and Hoechst33342 (Dojindo Laboratories) for 1 h at
199	room temperature. After washing three times with PBS and once with distilled water,
200	samples were mounted on slides and examined by using a LSM-710 confocal
201	laser-scanning microscope (Carl Zeiss). Images of single confocal planes are presented.
202	
203	Single-cell intensity analysis. Neurospheres on day 18 were dissociated into single cells
204	and re-plated on coverslips for 5 hours; then, they were fixed, immunolabeled, and
205	imaged as described above. Randomly selected three representative images were
206	analyzed by ImageJ. First, the nuclear areas were identified by Hoechst staining that
207	was larger than 50 μm^2 in surface area and with intensity levels that were typical and
208	lower than the threshold brightness of pyknotic cells. Next, the 8-bit grayscale intensity
209	values of the intended markers were measured in each nuclear area.

210		

211	Cleaved CASPASE3 analysis. Stained coverslips were imaged on the high-content
212	cellular analysis system IN Cell Analyzer 6000 (GE Healthcare). Analysis using IN Cell
213	Developer Toolbox v1.9 (GE Healthcare) began by identifying intact nuclei stained by
214	Hoechst dye, which were defined as traced nuclei that were larger than 50 μm^2 in
215	surface area and with intensity levels that were typical and lower than the threshold
216	brightness of pyknotic cells. Each traced nuclear region was then expanded by 50% to
217	mark the cell soma region and cross-referenced with neuronal subtype markers (HB9,
218	CTIP2, OTX1, FOXP2, and SOX1). Using the traced images for each cell, the number
219	of the cleaved CASPASE3-positive products within the specific marker-positive or
220	-negative cells was quantified; then, its ratio to the number of the specific
221	marker-positive or -negative cells was reported.
222	
223	Microarray analysis. Total RNA from neurospheres on day 18 was extracted by
224	RNeasy Micro Kit (QIAGEN). 20 ng of total RNA was converted into amplified cDNA
225	by using Ovation Pico WTA System V2 (NuGEN) and labeled by using the SureTag

226	Complete DNA Labeling Kit (Agilent). The labeled cDNA was hybridized to SurePrint
227	G3 Human GE v3 8 \times 60K Microarrays (Agilent). The scanned images were analyzed
228	with Feature Extraction Software 12.0.3.1 (Agilent) using default parameters to obtain
229	background-subtracted and spatially detrended processed signal intensities. Expression
230	was quantile normalized, and corrected for chip batch effect via ComBat (Johnson et al.,
231	2007). Data were log-transformed and ANOVA with error variance averaging was
232	performed with the NIA Array Analysis Tool (Sharov et al., 2005). We used the
233	maximum of actual error variance and error variance averaged across 500 genes with
234	similar average expression as the denominator of F-statistic. Probes with top 1% of
235	error variances were not used for the error variance averaging. F-statistic is then used to
236	estimate the P-value according to theoretical F-distribution.
237	The microarray dataset has been deposited in the NCBI Gene Expression Omnibus
238	and is accessible through GEO series accession number GSE111106.
239	
240	Correlation analysis between different gene expression datasets. The microarray data
241	for 9-11 pcw macro-dissected human fetal brains (Ip et al., 2010) were downloaded

242	from ArrayExpress (E-MEXP-2700), normalized using fRMA (McCall et al., 2010).
243	The RNA-seq data (FPM values) of 12 and 13 pcw micro-dissected human fetal brains
244	were obtained from the BrainSpan database (BrainSpan, 2017) and quantile normalized.
245	We compared our microarray dataset with these datasets with ExAtlas software (Sharov
246	et al., 2015). First, data were preprocessed by log-transformation and removing outliers
247	(z-value \geq 8). We performed ANOVA in each dataset with error variance averaging as
248	described above. In the case of our microarray dataset, all samples were analyzed as
249	individual factors, and the error variance is estimated based on the half-normal
250	probability plot method. The P-values were transformed to FDR using the
251	Benjamini-Hochberg method. We identified genes with significant change of expression
252	(FDR \leq 0.05, fold change \geq 4) in each dataset, estimated gene expression change
253	relative to median expression, and calculated a z-value of Pearson's correlation for the
254	subset of common significant genes. Clustering analysis was performed using complete
255	linkage clustering and Euclidean distance.

- 257 Experimental design and statistical analysis. All data were expressed as the mean \pm
- 258 SEM. Statistical analyses were performed using one-way ANOVA followed by post hoc
- 259 Dunnett's or Tukey's test for multiple comparisons. ANOVA with error variance
- 260 averaging was performed in the transcriptome analysis as described above.

261 Results

262	Expression change of R-C marker genes by modulating FGF8 signaling
263	The gradient of FGF8 signaling along the R-C axis establishes the areal identity in the
264	developing cerebral cortex in mice (Fukuchi-Shimogori and Grove, 2001). We
265	hypothesized that the R-C identity of neural progenitors differentiated from PSCs can
266	be controlled by regulating FGF8 signaling, leading to the establishment of areal
267	identity across the frontal, parietal, temporal, and occipital lobes (Fig. 1A).
268	We previously demonstrated that PSCs acquire cerebral cortical identity by
269	inhibiting Wnt signaling during neural induction (Imaizumi et al., 2015). We utilized
270	this protocol and generated neurospheres with the cerebral cortical identity derived from
271	ESCs by treatment with the Wnt inhibitor IWR1e. FGF8 signaling was then modulated
272	by applying recombinant FGF8 protein or soluble FGF receptor 3 (sFGFR3), which
273	sequesters endogenous FGF8 (Fig. 1B).
274	The treatment with FGF8 or sFGFR3 maintained FOXG1 expression, indicating that
275	fluctuations in FGF8 signaling levels did not alter the cortical identity; rather, FGF8
276	slightly upregulated FOXG1 expression, as has previously been shown in mouse

277	embryos (Shimamura and Rubenstein, 1997) (Fig. 2A). As FGF8 signaling was
278	activated, the rostral markers SP8 and PEA3 (Fukuchi-Shimogori and Grove, 2003;
279	Sahara et al., 2007) were highly expressed, whereas the caudal markers COUP-TFI and
280	FGFR3 (Zhou et al., 2001; Hébert et al., 2003) were downregulated (Fig. 2A). These
281	gene expression changes were also confirmed by immunocytochemical analysis for the
282	SP8 and COUP-TFI proteins (Fig. 2B and C). It should be noted that untreated and
283	FGF8-treated cells expressed low levels of SP8 and COUP-TFI, respectively. This
284	result is consistent with the fact that the cortical regional marker genes are expressed in
285	a graded manner, which is different from the clearly delineated, distinct expression
286	pattern in other brain regions (Sansom and Livesey, 2009). Overall, our results suggest
287	that R-C marker expression can be controlled by modulating FGF8 signaling during
288	neurosphere formation from human PSCs.
289	
290	Transcriptome profiling and comparison with human fetal brains
291	To further investigate R-C identity, we performed gene expression profiling by

microarray analysis. The rostral and caudal markers were enriched in FGF8-treated and

293	untreated cells, respectively (Fig. 3A). A comparison of these data with those from
294	human fetal brains dissected as 5-mm coronal slices along the R-C axis (Ip et al., 2010)
295	showed that FGF8-treated cells more closely matched the rostral areas while showing
296	less similarity to the middle and caudal areas (Fig. 3B). To characterize the areal
297	identity in more detail, our microarray data were next compared with the RNA-seq data
298	from micro-dissected brains of human embryos from the BrainSpan database
299	(BrainSpan, 2017). This analysis demonstrated that untreated cells were best correlated
300	with the temporal lobe, while FGF8-treated cells most closely resembled the
301	sensorimotor cortex (Fig. 3C). Collectively, these data indicate that the global gene
302	expression patterns of PSC-derived neural progenitors were shifted toward a rostral fate
303	by the activation of FGF8 signaling.
304	
305	Cortical neurons with rostral identity exhibited ALS phenotypes
306	ALS affects both upper motor neurons (UMNs) and lower motor neurons (LMNs) (Fig.
307	4A); however, PSC-based disease modeling has been successfully achieved only in
308	LMN phenotypes because UMN derivation protocols have never been established

309	(Sances et al., 2016). As our data indicated that FGF8-treated cells correspond to the
310	primary motor cortex, we hypothesized that these cells can elucidate UMN phenotypes.
311	To test this hypothesis, we used iPSC lines from two kinds of familial ALS: ALS2 and
312	ALS6, carrying ALS2 or FUS mutations, respectively (Shirakawa et al., 2009; Akiyama
313	et al., 2016). These cells were differentiated into neurons by adapting the above
314	protocol or an LMN derivation method as previously described (Imaizumi et al., 2015)
315	(Fig. 4B). We observed increased cleaved CASPASE3 activity in HB9-expressing
316	LMNs derived from FUS-mutated iPSCs compared with those from healthy control
317	ESC/iPSC lines, as was shown in a previous study (Ichiyanagi et al., 2016); however,
318	such phenotypes were absent in ALS2-mutated cells (Fig. 4C and D). On the other hand,
319	FGF8-treated forebrain neurons derived from ALS2-mutated iPSCs showed increased
320	apoptosis, while there were no changes in untreated cells (Fig. 4E and F). FUS-mutated
321	forebrain neurons did not exhibit such phenotypes in either untreated or FGF8-treated
322	cultures. These data suggest that an ALS2 mutation enhances apoptosis only in forebrain
323	neurons with rostral identity. Importantly, this phenotype was observed only in cells
324	labeled with CTIP2, a marker for layer V subcerebral projection neurons, indicative of

325	UMN-specific vulnerability (Molyneaux et al., 2007). The UMN selectivity of this
326	phenotype is also supported by the fact that cells positive for OTX1, another layer V
327	maker, showed increased apoptosis, whereas FOXP2-positive layer VI corticothalamic
328	neurons did not (Molyneaux et al., 2007) (Fig. 4G and H). Finally, to assess whether
329	this cell death vulnerability is also observed in the developmental stage, SOX1-positive
330	neural progenitors in neurospheres were analyzed for apoptosis. FGF8-treated and
331	untreated neural progenitors displayed no changes in apoptosis (Fig. 4I and J). Overall,
332	selective cell death was observed in layer V cortical neurons with the rostral identity
333	derived from ALS2-mutated iPSCs, suggesting that UMN phenotypes of ALS were
334	recapitulated.

335 Discussion

336	In this study, we established a culture system to control the R-C identity of PSC-derived
337	cortical neurons by regulating FGF8 signaling. FGF8 activation converted the cell fate
338	from caudal (the temporal lobe) to rostral (the sensorimotor cortex). Moreover, the
339	area-specific forebrain phenotypes of ALS2-associated ALS were reproduced in vitro by
340	using this system.
341	The gradient of morphogens, such as FGFs, Wnts, and BMPs, determines the areal
342	identity during neural development (O'Leary et al., 2007). Of these signaling molecules,
343	FGF8 has been most studied as a central regulator of cortical area patterning. FGF8 is
344	secreted from ANR, which is located in the rostral-most part of the neural tube,
345	establishes a gradient along the R-C axis, and modulates the expression of transcription
346	factors that specify the areal identity (Fukuchi-Shimogori and Grove, 2003; Toyoda et
347	al., 2010). Our primary aim was in vitro recapitulation of this mechanism by using
348	PSCs. In fact, it has previously been reported that FGF8 treatment changes the R-C
349	marker expression in mouse and human PSC-derived neurons (Eiraku et al., 2008;
350	Kadoshima et al., 2013); however, these studies examined the expression of only a few

351	markers. In contrast, we investigated the areal identity in more detail by comparing the
352	global gene expression profile with that of fetal brains in the existing databases. Our
353	data confirm and extend these previous reports and suggest that the areal patterning can
354	be precisely controlled in human PSC cultures.
355	The protocols to produce subcerebral projection neurons in the primary motor
356	cortex, or UMNs, from PSCs have not yet been established, hindering the prospect of
357	modeling the pathogenesis of ALS in vitro (Sances et al., 2016). We challenged this
358	problem by using our culture protocol. In these experiments, we chose ALS2-mutated
359	iPSCs as a source because the mutation of ALS2 that we used results in UMN-dominant
360	symptoms (Shirakawa et al., 2009) and ALS2 is also known to be a causative gene for
361	other UMN diseases, such as primary lateral sclerosis (PLS) and hereditary spastic
362	paraplegia (HSP) (Chandran et al., 2007; Otomo et al., 2012). It is noteworthy that the
363	observed phenotypes were both area-specific and layer-specific. This double selectivity
364	increased the reliability of our claim that UMN phenotypes can be recapitulated in our
365	culture system. On the other hand, FUS-mutated cells showed only LMN phenotypes in
366	our culture system, consistent with the fact that this patient exhibited LMN symptoms at

367	onset, preceding that of UMN, and that these are not complicated by other
368	forebrain-associated symptoms, such as frontotemporal dementia (FTD) (Akiyama et al.,
369	2016). These results indicate that our culture system recapitulated well the clinical
370	manifestation of ALS2- and FUS-associated ALS. The difference in the observed
371	phenotypes between these two types of ALS suggests that ALS pathogenesis can be
372	divided into two groups: one predominantly affects UMNs, and the other preferentially
373	disturbs LMNs. Although the mechanism of the selectivity of ALS phenotypes is still
374	unclear, our system now offers new opportunities to clarify this mechanism.
375	Before perfect control of the areal identity of PSC-derived neurons can be
376	demonstrated, there are some remaining issues to be resolved: (i) hodological
377	characterization in transplantation experiments and (ii) the requirement for signaling
378	cues in addition to FGF8. The areal identity is characterized not only by gene
379	expression patterns but also by hodological properties. In previous studies, when grafted
380	into the mouse cortex, mouse and human PSC-derived neurons displayed specific
381	patterns of axonal projections corresponding to the visual cortex, which indicates that
382	these cells retain the identity of this cortical area (Gaspard et al., 2008;

384	on areal identity.
385	In addition to FGF8, Wnts and BMPs also regulate areal patterning. These
386	morphogens are secreted from the cortical hem, positioned at the medial edge of the
387	cortex, and define areal identity (Caronia-Brown et al., 2014). A previous study showed
388	that PSCs can be specified to differentiate into hippocampal neurons by activating Wnt
389	and BMP signaling (Sakaguchi et al., 2015). In another study, inhibition of Wnt
390	signaling induced rostral marker expression (Motono et al., 2016). The modulation of
391	these signaling pathways, along with that of FGF8, will enable finer control of areal
392	identity in PSC cultures. Additionally, other, currently unknown, signaling pathways
393	may have an effect on areal patterning. FGF8-treated cells in our culture system
394	acquired a rostral identity but showed similarity to the sensorimotor cortex, rather than
395	the prefrontal cortex. Although it is probable that a higher concentration of FGF8 is
396	necessary for the specification of the prefrontal cortex, another possibility is that
397	additional signaling molecules are required. As the prefrontal cortex has markedly
398	expanded through evolution, it is worth considering the hypothesis that a novel

383 Espuny-Camacho et al., 2013). Such transplantation experiments will reinforce our data

- 399 morphogen for prefrontal area patterning has emerged in human evolution. Our culture
- 400 system using human PSCs will allow for the study of such human-specific
- 401 neurodevelopmental processes.

REFERENCES

403	Akiyama T, Warita H, Kato M, Nishiyama A, Izumi R, Ikeda C, Kamada M, Suzuki N,
404	Aoki M (2016) Genotype-phenotype relationships in familial amyotrophic lateral
405	sclerosis with FUS/TLS mutations in Japan. Muscle Nerve 54:398-404.
406	BrainSpan (2017) BrainSpan atlas of the developing human brain. Available at:
407	http://www.brainspan.org.
408	Caronia-Brown G, Yoshida M, Gulden F, Assimacopoulos S, Grove EA (2014) The
409	cortical hem regulates the size and patterning of neocortex. Development 141:2855-
410	2865.
411	Chandran J, Ding J, Cai H (2007) Alsin and the molecular pathways of amyotrophic
412	lateral sclerosis. Mol Neurobiol 36:224-231.
413	Eiraku M, Watanabe K, Matsuo-Takasaki M, Kawada M, Yonemura S, Matsumura M,
414	Wataya T, Nishiyama A, Muguruma K, Sasai Y (2008) Self-Organized Formation
415	of Polarized Cortical Tissues from ESCs and Its Active Manipulation by Extrinsic
416	Signals. Cell Stem Cell 3:519–532.
417	Espuny-Camacho I, Michelsen KA, Gall D, Linaro D, Hasche A, Bonnefont J, Bali C,
418	Orduz D, Bilheu A, Herpoel A, Lambert N, Gaspard N, Péron S, Schiffmann SN,
419	Giugliano M, Gaillard A, Vanderhaeghen P (2013) Pyramidal Neurons Derived
420	from Human Pluripotent Stem Cells Integrate Efficiently into Mouse Brain Circuits
421	In Vivo. Neuron 77:440–456.
422	Fukuchi-Shimogori T, Grove EA (2001) Neocortex patterning by the secreted signaling
423	molecule FGF8. Science 294:1071-1074.
424	Fukuchi-Shimogori T, Grove EA (2003) Emx2 patterns the neocortex by regulating FGF
425	positional signaling. Nat Neurosci 6:825-831.
426	Gaspard N, Bouschet T, Hourez R, Dimidschstein J, Naeije G, van den Ameele J,
427	Espuny-Camacho I, Herpoel A, Passante L, Schiffmann SN, Gaillard A,
428	Vanderhaeghen P (2008) An intrinsic mechanism of corticogenesis from embryonic
429	stem cells. Nature 455:351–357.
430	Hébert JM, Lin M, Partanen J, Rossant J, McConnell SK (2003) FGF signaling through
431	FGFR1 is required for olfactory bulb morphogenesis. Development 130:1101–1111.
432	Ichiyanagi N, Fujimori K, Yano M, Ishihara-Fujisaki C, Sone T, Akiyama T, Okada Y,
433	Akamatsu W, Matsumoto T, Ishikawa M, Nishimoto Y, Ishihara Y, Sakuma T,

434	Yamamoto T, Tsuiji H, Suzuki N, Warita H, Aoki M, Okano H (2016)
435	Establishment of in Vitro FUS-Associated Familial Amyotrophic Lateral Sclerosis
436	Model Using Human Induced Pluripotent Stem Cells. Stem Cell Reports 6:496-510.
437	Imaizumi K, Sone T, Ibata K, Fujimori K, Yuzaki M, Akamatsu W, Okano H (2015)
438	Controlling the Regional Identity of hPSC-Derived Neurons to Uncover Neuronal
439	Subtype Specificity of Neurological Disease Phenotypes. Stem Cell Reports
440	5:1010–1022.
441	Imaizumi Y, Okano H (2014) Modeling human neurological disorders with induced
442	pluripotent stem cells. J Neurochem 129:388-399.
443	Ip BK, Wappler I, Peters H, Lindsay S, Clowry GJ, Bayatti N (2010) Investigating
444	gradients of gene expression involved in early human cortical development. J Anat
445	217:300–311.
446	Johnson WE, Li C, Rabinovic A (2007) Adjusting batch effects in microarray expression
447	data using empirical Bayes methods. Biostatistics 8:118-127.
448	Kadoshima T, Sakaguchi H, Nakano T, Soen M, Ando S, Eiraku M, Sasai Y (2013)
449	Self-organization of axial polarity, inside-out layer pattern, and species-specific
450	progenitor dynamics in human ES cell-derived neocortex. Proc Natl Acad Sci U S A
451	110:20284–20289.
452	Lippmann ES, Williams CE, Ruhl DA, Estevez-silva MC, Chapman ER, Coon JJ, Ashton
453	RS (2015) Deterministic HOX Patterning in Human Pluripotent Stem Cell-Derived
454	Neuroectoderm. Stem Cell Reports 4:1–13.
455	Lu J, Zhong X, Liu H, Hao L, Huang CT-L, Sherafat MA, Jones J, Ayala M, Li L, Zhang
456	S-C (2015) Generation of serotonin neurons from human pluripotent stem cells. Nat
457	Biotechnol 34:89–94.
458	Marchetto MC, Gage FH (2012) Modeling brain disease in a dish: really? Cell Stem Cell
459	10:642–645.
460	Maroof AM, Keros S, Tyson J a, Ying S-W, Ganat YM, Merkle FT, Liu B, Goulburn A,
461	Stanley EG, Elefanty AG, Widmer HR, Eggan K, Goldstein P a, Anderson S a,
462	Studer L (2013) Directed differentiation and functional maturation of cortical
463	interneurons from human embryonic stem cells. Cell Stem Cell 12:559-572.
464	Mattis VB, Svendsen CN (2011) Induced pluripotent stem cells: A new revolution for
465	clinical neurology? Lancet Neurol 10:383-394.

	466	McCall MN, Bolstad BM, Irizarry RA (2010) Frozen robust multiarray analysis (fRMA).
	467	Biostatistics 11:242–253.
	468	Molyneaux BJ, Arlotta P, Menezes JRL, Macklis JD (2007) Neuronal subtype
	469	specification in the cerebral cortex. Nat Rev Neurosci 8:427-437.
	470	Motono M, Ioroi Y, Ogura T, Takahashi J (2016) WNT-C59, a Small-Molecule WNT
f	471	Inhibitor, Efficiently Induces Anterior Cortex That Includes Cortical Motor Neurons
	472	From Human Pluripotent Stem Cells. Stem Cells Transl Med 5:552-560.
<u> </u>	473	Muguruma K, Nishiyama A, Kawakami H, Hashimoto K, Sasai Y (2015)
C	474	Self-Organization of Polarized Cerebellar Tissue in Article Self-Organization of
\sim	475	Polarized Cerebellar Tissue in 3D Culture of Human Pluripotent Stem Cells.
\supset	476	CellReports 10:1–14.
o Accepted Manuscript	477	O'Leary DDM, Chou S, Sahara S (2007) Area Patterning of the Mammalian Cortex.
σ	478	Neuron 56:252–269.
	479	Okada Y, Matsumoto A, Shimazaki T, Enoki R, Koizumi A, Ishii S, Itoyama Y, Sobue G,
\leq	480	Okano H (2008) Spatiotemporal recapitulation of central nervous system
	481	development by murine embryonic stem cell-derived neural stem/progenitor cells.
	482	Stem Cells 26:3086–3098.
	483	Okada Y, Shimazaki T, Sobue G, Okano H (2004)
	484	Retinoic-acid-concentration-dependent acquisition of neural cell identity during in
	485	vitro differentiation of mouse embryonic stem cells. Dev Biol 275:124-142.
U U	486	Okano H, Yamanaka S (2014) iPS cell technologies: significance and applications to
\mathbf{O}	487	CNS regeneration and disease. Mol Brain 7:22.
	488	Otomo A, Pan L, Hadano S (2012) Dysregulation of the autophagy-endolysosomal
	489	system in amyotrophic lateral sclerosis and related motor neuron diseases. Neurol
0	490	Res Int 2012:498428.
	491	Sahara S, Kawakami Y, Izpisua Belmonte J, O'Leary DD (2007) Sp8 exhibits reciprocal
	492	induction with Fgf8 but has an opposing effect on anterior-posterior cortical area
	493	patterning. Neural Dev 2:10.
	494	Sakaguchi H, Kadoshima T, Soen M, Narii N, Ishida Y, Ohgushi M, Takahashi J, Eiraku
eNeur	495	M, Sasai Y (2015) Generation of functional hippocampal neurons from
Ð	496	self-organizing human embryonic stem cell-derived dorsomedial telencephalic
	497	tissue. Nat Commun 6:8896.

198	Sances S, Bruijn LI, Chandran S, Eggan K, Ho R, Klim JR, Livesey MR, Lowry E,
199	Macklis JD, Rushton D, Sadegh C, Sareen D, Wichterle H, Zhang S-C, Svendsen
500	CN (2016) Modeling ALS with motor neurons derived from human induced
501	pluripotent stem cells. Nat Neurosci 16:542-553.
502	Sansom SN, Livesey FJ (2009) Gradients in the brain: the control of the development of
503	form and function in the cerebral cortex. Cold Spring Harb Perspect Biol 1:a002519.
504	Seki T, Yuasa S, Oda M, Egashira T, Yae K, Kusumoto D, Nakata H, Tohyama S,
505	Hashimoto H, Kodaira M, Okada Y, Seimiya H, Fusaki N, Hasegawa M, Fukuda K
506	(2010) Generation of induced pluripotent stem cells from human terminally
507	differentiated circulating t cells. Cell Stem Cell 7:11-13.
508	Sharov AA, Dudekula DB, Ko MSH (2005) A web-based tool for principal component
509	and significance analysis of microarray data. Bioinformatics 21:2548-2549.
510	Sharov AA, Schlessinger D, Ko MSH (2015) ExAtlas: An interactive online tool for
511	meta-analysis of gene expression data. J Bioinform Comput Biol 13:1550019.
512	Shimamura K, Rubenstein JL (1997) Inductive interactions direct early regionalization of
513	the mouse forebrain. Development 124:2709-2718.
514	Shimazaki T, Shingo T, Weiss S (2001) The ciliary neurotrophic factor/leukemia
515	inhibitory factor/gp130 receptor complex operates in the maintenance of
516	mammalian forebrain neural stem cells. J Neurosci 21:7642-7653.
517	Shirakawa K, Suzuki H, Ito M, Kono S, Uchiyama T, Ohashi T, Miyajima H (2009)
518	Novel compound heterozygous ALS2 mutations cause juvenile amyotrophic lateral
519	sclerosis in Japan. Neurology 73:2124–2126.
520	Suemori H, Yasuchika K, Hasegawa K, Fujioka T, Tsuneyoshi N, Nakatsuji N (2006)
521	Efficient establishment of human embryonic stem cell lines and long-term
522	maintenance with stable karyotype by enzymatic bulk passage. Biochem Biophys
523	Res Commun 345:926–932.
524	Takahashi K, Tanabe K, Ohnuki M, Narita M, Ichisaka T, Tomoda K, Yamanaka S
525	(2007) Induction of pluripotent stem cells from adult human fibroblasts by defined
526	factors. Cell 131:861-872.
527	Tao Y, Zhang SC (2016) Neural Subtype Specification from Human Pluripotent Stem
528	Cells. Cell Stem Cell 19:573–586.

- 529 Toyoda R, Assimacopoulos S, Wilcoxon J, Taylor A, Feldman P, Suzuki-Hirano A,
- 530 Shimogori T, Grove EA (2010) FGF8 acts as a classic diffusible morphogen to
- 531 pattern the neocortex. Development 137:3439–3448.
- 532 Zhou C, Tsai SY, Tsai MJ (2001) COUP-TFI: an intrinsic factor for early regionalization
- 533 of the neocortex. Genes Dev 15:2054–2059.

536 Legends

537	Figure 1. Strategy for controlling the areal identity of PSC-derived neurons
538	(A) Schematic diagram of areal patterning in the cerebral cortex. The rostrocaudal
539	(R-C) gradient of FGF8 signaling determines areal identity.
540	(B) Overview of the culture protocol. FGF8 modulators (FGF8 and sFGFR3) were
541	added at the secondary neurosphere stage.
542	
543	Figure 2. Effect of FGF8 on R-C marker expression
544	(A) qRT-PCR analysis of ESC-derived neurospheres for R-C marker expression ($n = 3$;
545	mean \pm SEM; ***P < 0.001; **P < 0.01; *P < 0.05; ANOVA with Dunnett's test). The
546	concentration (ng/mL) of FGF8 is presented as a superscript.
547	(B) Representative immunofluorescent images for R-C markers (scale bar = $50 \ \mu m$).
548	(C) Histogram showing the distribution of the immunofluorescent intensity of SP8 and
549	COUP-TFI measured at the single-cell level.
550	

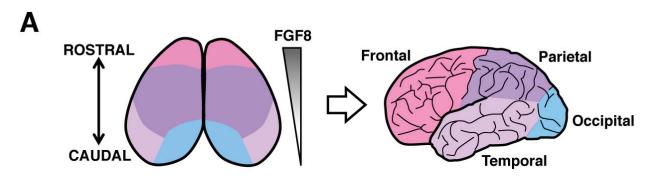
552 human fetal brains

553	(A) Volcano plot of the expression profile of FGF8-treated cells relative to control, with
554	differentially expressed genes (P < 0.05; Student's t test) highlighted (dark gray). The
555	rostral (red) and caudal (blue) markers were enriched in FGF8-treated and untreated
556	cells, respectively.
557	(B, C) Correlation matrix of the global gene expression with macro-dissected (B) and
558	micro-dissected (C) human fetal brains. FGF8-treated cells well correlated with the
559	rostral portions of macro-dissected brains and with the sensorimotor cortex of
560	micro-dissected brains. pcw, post-conception weeks; OFC, orbital prefrontal cortex;
561	MFC, mediolateral prefrontal cortex; DFC, dorsolateral prefrontal cortex; VFC,
562	ventrolateral prefrontal cortex; M1C, primary motor cortex; S1C, primary sensory
563	cortex; IPC, inferior parietal cortex; A1C, primary auditory cortex; STC, superior
564	temporal cortex; ITC, inferolateral temporal cortex; V1C, primary visual cortex.
565	
566	

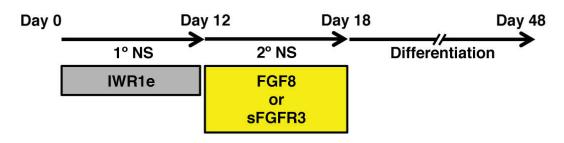
568 Figure 4. Recapitulation of ALS phenotypes in *FUS*- and *ALS2*-mutated cells

- 569 (A) Schematic diagram of motor neurons affected in ALS. UMN, upper motor neuron;
- 570 LMN, lower motor neuron.
- 571 (B) Overview of the LMN derivation protocol.
- 572 (C) Representative immunofluorescent images of apoptotic LMNs at day 42 (scale bar =
- 573 50 μm (upper); 10 μm (lower)). Arrowheads indicate the cleaved CASPASE3-positive
- 574 cells.
- 575 (D) Quantification of the cleaved CASPASE3-positive products in LMNs at day 42 (n =
- 576 3; mean \pm SEM; ***P < 0.001; **P < 0.01; ANOVA with Tukey's test). HB9-positive
- 577 LMNs derived from FUS-mutated cells selectively showed increased apoptosis.
- 578 (E) Representative immunofluorescent images of apoptotic cortical cells at day 48
- 579 (scale bar = $50 \mu m$ (upper); $10 \mu m$ (lower)). Arrowheads indicate the cleaved
- 580 CASPASE3-positive cells.
- 581 (F) Quantification of the cleaved CASPASE3-positive products in untreated and
- 582 FGF8-treated cortical cells at day 48 (n = 3-5; mean \pm SEM; ***P < 0.001; ANOVA

583	with Tukey's test). CTIP2-positive cortical cells derived from FGF8-treated
584	ALS2-mutated neurospheres selectively showed increased apoptosis.
585	(G) Representative immunofluorescent images of apoptotic cortical cells at day 48
586	(scale bar = 10 μ m). Arrowheads indicate the cleaved CASPASE3-positive cells.
587	(H) Quantification of the cleaved CASPASE3-positive products in untreated and
588	FGF8-treated cortical cells at day 48 (n = 4–5; mean \pm SEM; ***P < 0.001; ANOVA
589	with Tukey's test). OTX1-positive cortical cells, but not FOXP2-positive cells, derived
590	from FGF8-treated ALS2-mutated neurospheres selectively showed increased apoptosis.
591	(I) Representative immunofluorescent images of SOX1/cleaved CASPASE3 in neural
592	progenitors in neurospheres at day 18 (scale bar = $10 \ \mu m$).
593	(J) Quantification of the cleaved CASPASE3-positive products in untreated and
594	FGF8-treated SOX1-positive neural progenitors in neurospheres at day 18 ($n = 3$; mean
595	\pm SEM). Selective cell death was not observed in neural progenitors.
596	



В



eNeuro Accepted Manuscript

